Ghost Interference and the Airgun Depth Determination

YIH JENG[1]

(Received 12 October 1990; Revised 14 December 1990)

ABSTRACT

Ghost interference on small airgun signatures has been experimentally investigated. A vertical hydrophone array was designed to receive the airgun energy output at different hydrophone depths. The airgun signatures were Fourier transformed to analyze the dominant frequency energy distribution. It was found that dominant frequency energy variation versus airgun depth could be described by a parabolic function. This result provides a good explanation for some conflicting points proposed by previous investigators. The determination of an optimum airgun depth by this method is particularly valuable if seismic records are to be processed without deghosting. A simple ghost interference model is proposed to explain the airgun depth of greater energy output and the depth of the less bubble pulse effect. The optimum airgun depth should compromise between the ghost interference and the desired frequency band in the seismic survey.

1. INTRODUCTION

Ghosts are a special type of multiple reflections. In marine seismic surveys, ghosts are the energy that initially travelled upward and then was reflected downward at the surface of the water (Telford *et al.*, 1976). Ghost interferences are especially important in marine seismic surveys because of the strong reflection of the water surface. The seismic records usually are inevitably contaminated by the ghosts thus several deghosting techniques have been developed such as the filtering method and seismic record composition which are now well known and widely used (Hammond, 1962; Jovanovich *et al.*, 1983; Lindsey, 1960; Robinson and Treitel, 1980; Schneider *et al.*, 1964). However, deghosting a large number of seismic records is a very tedious, time consuming task (Vaage *et al.*, 1983). In many cases, the raw seismic data are used without deghosting for practical reasons. Therefore, to find a shot depth with minimum ghost interference or constructive interference from different sources is desirable.

The incident source energy and the reflected ghost energy have a 180° phase shift or half a wavelength difference at the air-water boundary, hence

[1] *Department of Earth Science, National Taiwan Normal University, 88, Sec. 5, Roosevelt Road, Taipei, Taiwan, R. O. C.*

the effective path difference between the direct wave and the ghost wave is $(\lambda/2+2D)$, where λ is the wavelength of the source wavelet and D is the depth of the source below the water surface. The interference of the ghost depends on the fraction of a wavelength represented by the effective path difference and the distance between the receiver and the water surface. The reasons are i) the effective path difference accounting for energy construction or cancellation and ii) the distance between the receiver and the water surface determining the development of the ghost because the source ghost appears to have the same amplitude, the opposite polarity, and a slight delay with respect to the direct wave only when observed from a great distance (Fricke *et al.*, 1985).

The seismic signal is made up of a range of frequencies; the interference of the ghost and the signal will vary for different frequency components. If D is small in comparison with the dominant wavelengths, appreciable signal cancellation will occur. However, at some depths the interference is constructive; for instance, at depths of 10 to 17 m the ghost energy is constructive with the primary signal for frequencies of 25 to 40 Hz which are the dominant frequencies for usual seismic sources (Telford *et al.*, 1976).

The ghost may not develop if the receiver is not far enough from the water surface. The direct wave energy is greater than the ghost energy because of the difference in the travel paths. The direct arrival and the ghost arrival appear to have the same amplitude only when observed from a great distance, or infinity.

This paper presents the ghost interference of a small airgun seismic source by calculating the dominant frequency variation at different airgun depths. The striking result is that some conflicting points regarding the energy content of the dominant frequencies with airgun depths may be resolved in this experiment. The depth for small airguns to produce the optimum constructive ghost interference in the dominant frequency band can also be determined in this experiment. It is believed that this method will be useful in finding an airgun depth which can attenuate the bubble noise and improve the seismic data.

2. BASIC THEORY

An airgun signature (pressure pulse) begins with an initial pulse that represents the initial shock wave caused by the opening of the airgun ports. The energy stored in the compressed air is radiated as a pressure pulse goes into the surrounding water. The seismic signal is not, however, terminated with this initial pulse. The highly accelerated air particles expand beyond the state of equilibrium and reach a maximum radius larger than the equilibrium radius. After the air particles cease expanding, the surrounding water pressure compresses the air bubble until it again attains a high pressure. Thus the cycle of expansion and compression repeats continually with oscillations of diminishing

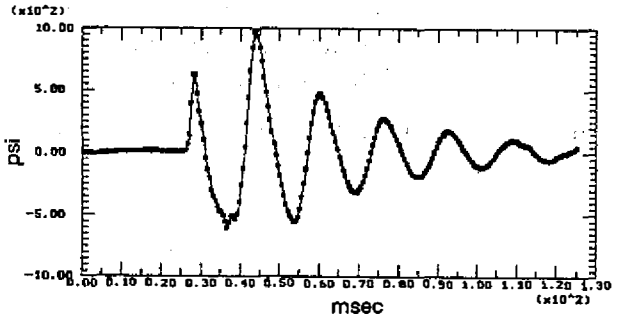

Fig. 1. Airgun signature (with ghost).

amplitude. In this way a train of bubble pulses is added to the signature of the initial pulse. The simple initial pulse becomes a long, oscillatory train. Figure 1 shows a typical airgun signature with its ghost.

The bubble oscillation is troublesome when recording the seismic record because it degrades the quality of the seismic data. In dealing with the bubble oscillation problem, it has been found that the use of an airgun array can attenuate the bubble pulses (Giles and Johnston, 1973; Johnston, 1980). For single airguns or guns of the same size, the bubble pulses can not be removed without the use of an inverse filter in data processing. A possible alternative for attenuating the bubble pulses would be the ghost interference described by this paper.

The period of the bubble oscillation can be obtained from:

$$T_b = K\frac{P^{1/3}\,V^{1/3}}{(D+10)^{5/6}} \qquad \text{(Brandsaeter } et\ al.\text{, 1979; Kramer } et\ al.\text{, 1968)} \quad (1)$$

where

T_b = bubble period in seconds,

P = ambient pressure at the firing depth in bars,

V = volume of the airgun chamber in cubic meters,

D = firing depth of the airgun in meters,

K = empirical constant depending on the type of airguns.

Theoretically, as the airgun depth increases, the separation time between the direct and ghost pressure waves becomes longer, and it is very likely that the ghost waves may cancel out the energy of direct waves on the following bubble pulses. Because the bubble period T_b depends on the type of airguns

and the airgun signature is made up of a range of component waves of different frequencies, the depth of the airgun which would obtain the least bubble pulse energy can only be obtained by field experiments.

The ghost energy will reinforce the source energy if there is no phase change at the boundary and

$$\frac{2D}{\lambda} = k, \qquad k = 0, 1, 2, \ldots \tag{2}$$

where

D = depth of the airgun or the receiver, depending on which one is located above the other,

λ = wavelength of the seismic wave.

Because

$$f\lambda = v,$$

where

f = frequency of the seismic wave,

v = velocity of the seismic wave,

therefore

$$\frac{2D}{v/f} = k. \tag{3}$$

At the air-water boundary the ghost waves are phase inverted, i.e., 180° phase shift; the energy received at the hydrophone will have troughs in the signature spectrum at frequencies of

$$f = k\frac{v}{2D} \tag{4}$$

because of the destructive interference of ghosts at those frequencies.

Actually, the shape of the ghost wavelet may be somewhat different from the primary wavelet because of the inhomogeneity of the material between the source and the free surface and because of the sphericity of the incident wavefront at the surface. The interference effects, which are the result of the uneven amplification for different frequency components of the seismic wave, are caused

by the inhomogeneity of the media between the source and the free surface boundary. The sphericity of the incident wavefront may produce a ray path somewhat modified from that assumed in the wave reflection.

3. EXPERIMENTAL

PAR (Trade mark of Bolt Associates, Inc.) 600B airguns with a chamber volume of 1.4 *cu.in.* were used throughout the experiment. A modified SIE RS-4 seismograph was used to amplify, filter, digitize, and record the data on PC floppy disks. The sampling interval was 0.5 *msec*, and the anti-aliasing filter was high-cut at 1,000 *Hz*. Six calibrated hydrophones were arranged vertically with 15 *meter* spacing between two adjacent hydrophones. This configuration made the experiment more efficient and minimize airgun signature variation from different shots, because the energy of one airgun discharge could reach six hydrophones at different depths. This experiment was carried out under static condition, i.e. without any vessel movement. The vessel's engine was shut down, and the hydrophones were kept at least 7 m away from the vessel to minimize vessel noise as much as possible. The cables that held the gun and the hydrophone array were suspended about 15 m from each other and about 7 m away from the vessel to avoid the cavitation problem and the effective afterflow range.

In this experiment, ocean current and wind are two major factors that affect the geometry of the vertical hydrophone array. In order to correct the positions of the airgun and hydrophones, a simple graphic method was used: The first hydrophone was only 1 *meter*, at most, down below the sea surface which is very close to the sea surface and thus could be treated as a point of fixed depth. From the first arrival at the first hydrophone, one could calculate the distance between the gun and the first hydrophone as S. Since the first hydrophone was treated as a fixed point O, a circle with center O and radius S was drawn to represent every possible position of the airgun. (In fact only a small arc of the circle below the sea surface was possible.) Therefore the length of the airgun cable below the sea surface, S', was used as the radius and the point O' where the airgun cable entered the sea water as the center to draw a second circle. The intersection of the two circles in the underwater region is the corrected position of the airgun. The positions of the other hydrophones relative to the airgun could be corrected by using the first arrivals and the spacing between adjacent hydrophones by the same graphic method: The first arrival was used to calculate the distance between airgun and hydrophone, the corrected airgun position was employed as the center, and the distance between airgun and hydrophone was taken as the radius to draw a circle. Another circle was determined with the previous hydrophone position as the center and the hydrophone spacing as the radius. The intersection of the two circles, which

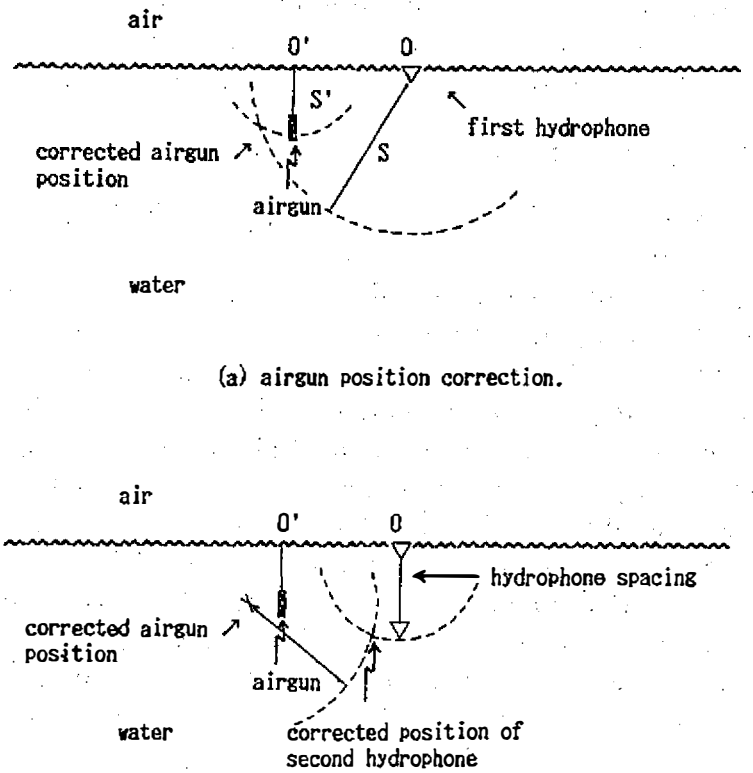

Fig. 2. The graphic method for the airgun and hydrophone position correction.

is below the position of the previous hydrophone, was the position of the next hydrophone (Fig. 2).

The first arrival is relatively critical in determining the geometry. The uncertainty for picking out the first arrivals is between ± 0.5 *msec* and ± 1.0 *msec* on the average. This comes mainly from the estimate of the delay time which is a combined effect of the function of electronic devices and airgun operation. Experience has shown that small airguns ranging from 1 *cu.in.* to 40 *cu.in.* have a 10 *msec* delay between trigger signal and air discharge. Other factors contributing to the uncertainty could be the accuracy limitation due to the sampling interval, 0.5 *msec* in this experiment for example, the position of airgun cable and hydrophone array at the sea surface. In actual data processing a range of up to ± 1.0 *msec* for the first arrival was tried before an optimized true geometry could be obtained. The airgun and hydrophone depths obtained from the true geometry have about 1 *m* difference for the airgun depth, 10 *m* difference at most for the hydrophone depth as compared to the original setup.

4. DATA ANALYSIS

Figures 3 to 8 are a series of typical spectrum variations for different airgun depths (D). The air pressure (P) used was 1000 *psi*, the airgun chamber volume (V) 1.4 *cu.in.*, and the nominal hydrophone depth (d) 31 m. The frequency axis of each figure ranges from 0 to 1000 Hz (Nyquist frequency) in order to show the dominant frequency band. These spectra are shown on the same graph in Fig. 9 for comparison. The frequency range in Fig. 9 is only up to 200 Hz because a frequency greater than 200 Hz is well beyond the dominant frequency band, which has little meaning in this comparison.

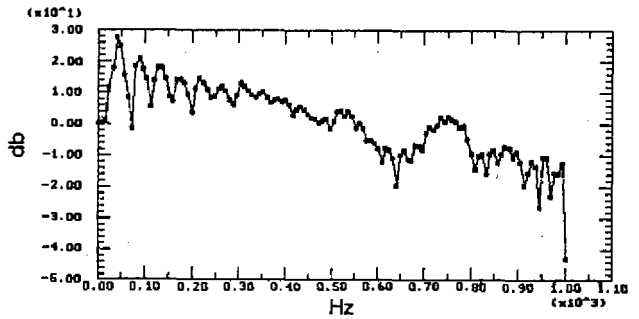

Fig. 3. Airgun signature spectrum: $P = 1000$ *psi*, $V = 1.4$ *cu.in.*, $d = 31$ m, $D = 2$ m.

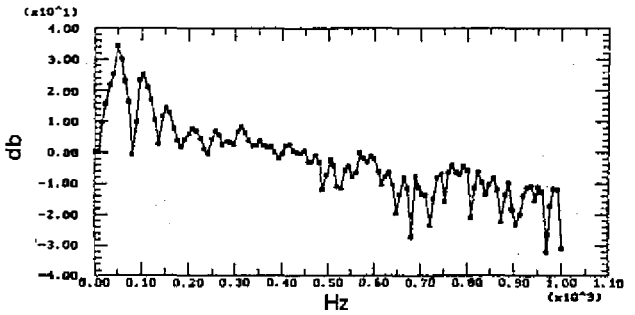

Fig. 4. Airgun signature spectrum: $P = 1000$ *psi*, $V = 1.4$ *cu.in.*, $d = 31$ m, $D = 4$ m.

The energy content of dominant frequencies of six different channels versus airgun depths is listed in Table 1. The energy content of the dominant frequency increases as airgun depth increases from 2 m to 8 m (or 1.5 m to 8 m after correction), then decreases at depths greater than 8 m (Table 1). The regression models for each channel are shown in Figs. 10 to 15.

The regression models show that a parabolic function may describe the variation of airgun energy with the airgun depth. There is a peak value of dominant frequency energy at an airgun depth of between 6 and 8 *meters*. This

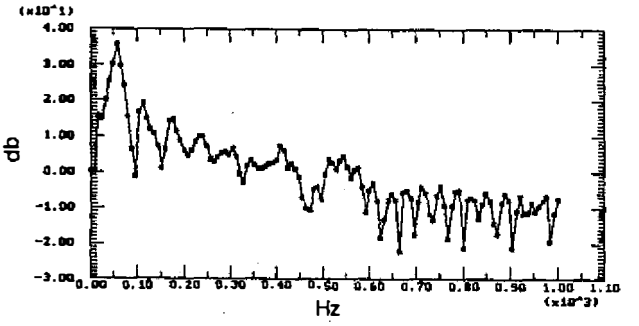

Fig. 5. Airgun signature spectrum: $P = 1000\ psi$, $V = 1.4\ cu.in.$, $d = 31\ m$, $D = 6\ m$.

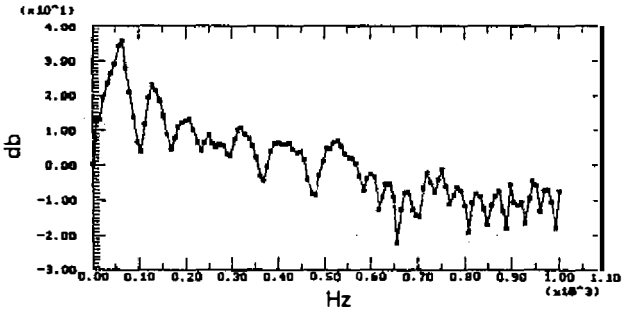

Fig. 6. Airgun signature spectrum: $P = 1000\ psi$, $V = 1.4\ cu.in.$, $d = 31\ m$, $D = 8\ m$.

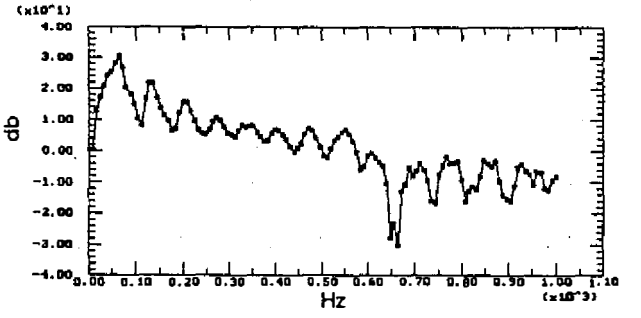

Fig. 7. Airgun signature spectrum: $P = 1000\ psi$, $V = 1.4\ cu.in.$, $d = 31\ m$, $D = 10\ m$.

phenomenon might provide a good explanation for the different experimental results obtained by Brandsaeter *et al.* (1979) and by Mayne and Quay (1971). Brandsaeter *et al.* found that the energy content increased in the dominant frequency band as the airgun depth increased. Their airgun depths ranged from 5 to 10 *meters*. Mayne and Quay obtained opposite results in their experiment. The airgun depths used by Mayne and Quay ranged from 7 to 13 *meters*. It appears that there could be an energy content peak for the dominant frequency band around an airgun depth of between 6 and 8 *meters*. For the spectrum en-

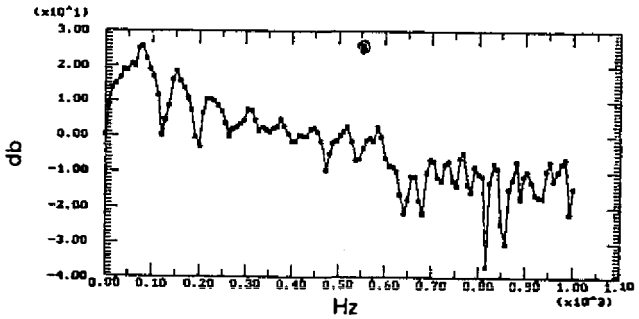

Fig. 8. Airgun signature spectrum: $P = 1000\ psi$, $V = 1.4\ cu.in.$, $d = 31\ m$, $D = 12\ m$.

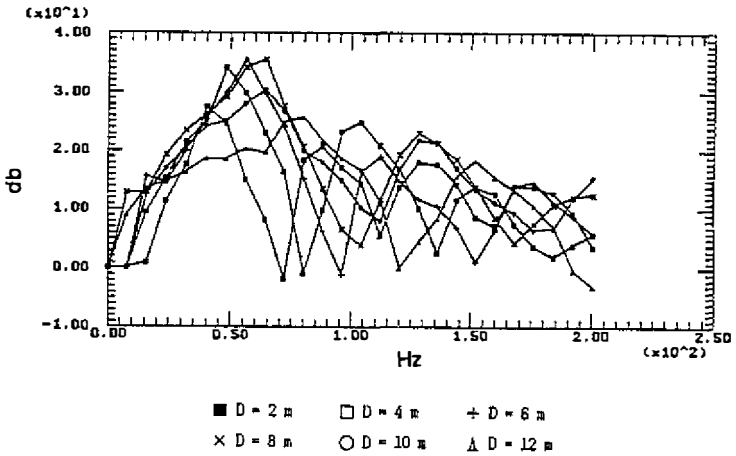

Fig. 9. Comparison of airgun signature spectra with different airgun depths ($P = 1000\ psi$, $V = 1.4\ cu.in.$, $d = 31\ m$).

Table 1. Dominant frequency energy content versus airgun and hydrophone depths.

Airgun depth	Channel 6 (1 m)	Channel 7 (16 m)	Channel 8 (31 m)	Channel 9 (46 m)	Channel 10 (61 m)	Channel 11 (76 m)
2 m *(1.5 m)	40.16 db (48 Hz)	38.70 db (40 Hz)	27.67 db (40 Hz)	31.79 db (40 Hz)	23.14 db (40 Hz)	15.02 db (40 Hz)
4 m *(4.0 m)	51.64 db (48 Hz)	49.77 db (48 Hz)	34.11 db (48 Hz)	36.02 db (48 Hz)	27.88 db (48 Hz)	21.49 db (48 Hz)
6 m *(6.0 m)	50.88 db (56 Hz)	51.10 db (56 Hz)	35.59 db (56 Hz)	36.26 db (56 Hz)	27.90 db (56 Hz)	21.06 db (56 Hz)
8 m *(8.0 m)	56.61 db (64 Hz)	55.71 db (64 Hz)	35.56 db (64 Hz)	40.48 db (64 Hz)	33.52 db (64 Hz)	26.68 db (64 Hz)
10 m *(9.5 m)	51.60 db (64 Hz)	49.28 db (64 Hz)	30.36 db (64 Hz)	29.97 db (64 Hz)	23.21 db (64 Hz)	16.26 db (64 Hz)
12 m *(12.0 m)	50.56 db (72 Hz)	42.61 db (72 Hz)	25.72 db (80 Hz)	27.39 db (80 Hz)	21.42 db (72 Hz)	15.20 db (80 Hz)

*airgun depth after correction

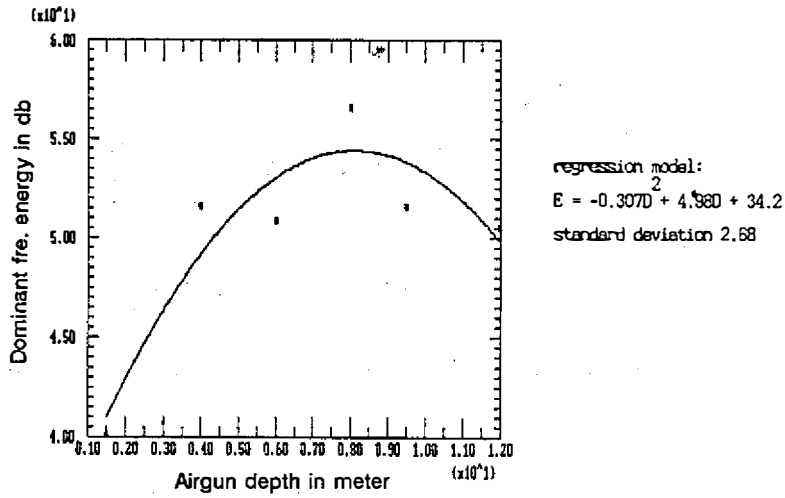

Fig. 10. Dominant frequency energy content E varying with airgun depth D (channel 6): $P = 1000\ psi$, $V = 1.4\ cu.in.$

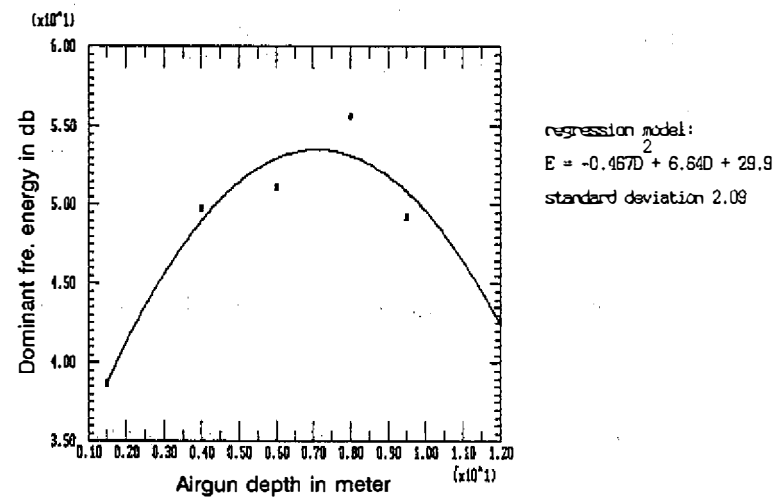

Fig. 11. Dominant frequency energy content E varying with airgun depth D (channel 7): $P = 1000\ psi$, $V = 1.4\ cu.in.$

ergy variation with airgun depth, Dragoset (1984) proposed that energy shifting is a combined effect of (1) the increased travel time separation between direct and ghost waves, (2) changes in the period and amplitude of the bubble oscillation, and (3) changes in the initial pressure pulse created by the gun. The first two effects are more likely in this experiment because the increased time separation between direct and ghost waves can reduce the energy cancellation between direct and ghost waves. As the airgun depth increases, the separation time gets longer, and it is very likely that the ghost waves begin to cancel out

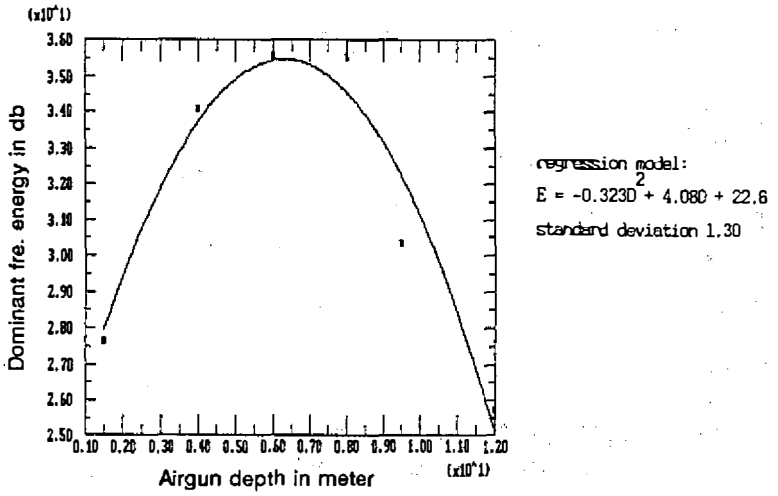

Fig. 12. Dominant frequency energy content E varying with airgun depth D (channel 8): $P = 1000\ psi$, $V = 1.4\ cu.in.$

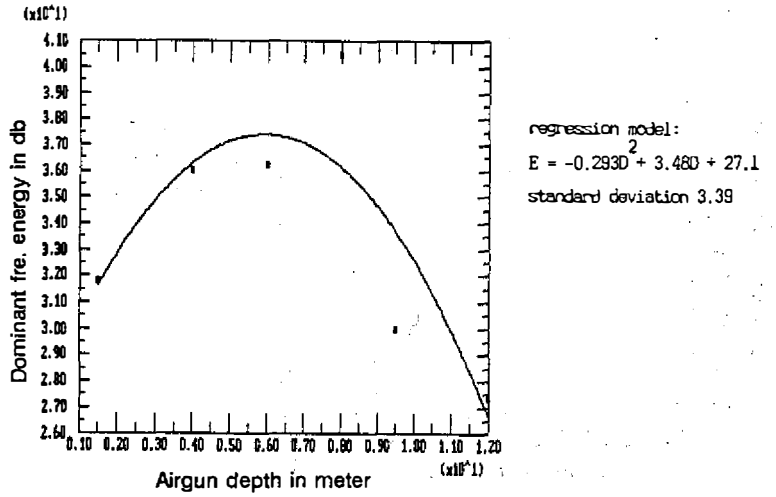

Fig. 13. Dominant frequency energy content E varying with airgun depth D (channel 9): $P = 1000\ psi$, $V = 1.4\ cu.in.$

the energy of direct waves on the following bubble pulses. Table 2 shows the measured initial pulse period (T_i), the measured bubble period (T_b), and the separation time (t_s) recorded by channel 8. The separation time (t_s) between direct and ghost waves can be obtained by calculating the difference of the direct wave path and the surface ghost path. Because the true airgun depth and the true hydrophone depth were determined by the above graphic method already, the surface ghost path was obtained by the simple reflection geometry.

Based on the value of the t_s/T_i ratio, a simple model is proposed in Fig. 16

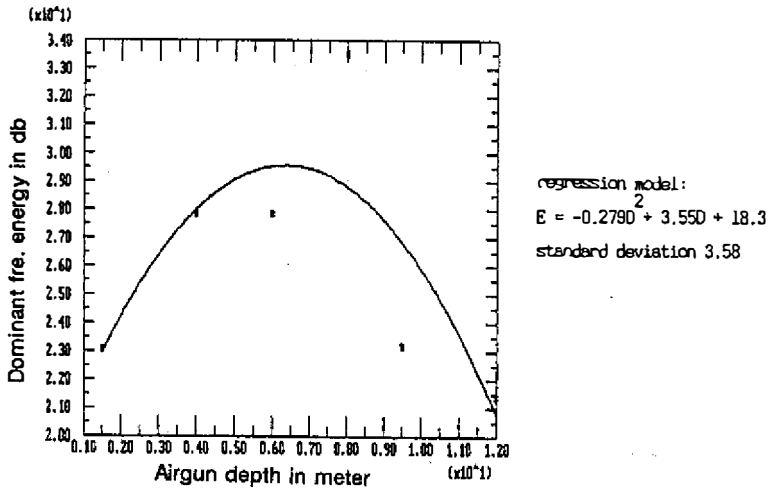

Fig. 14. Dominant frequency energy content E varying with airgun depth D (channel 10): $P = 1000\ psi$, $V = 1.4\ cu.in.$

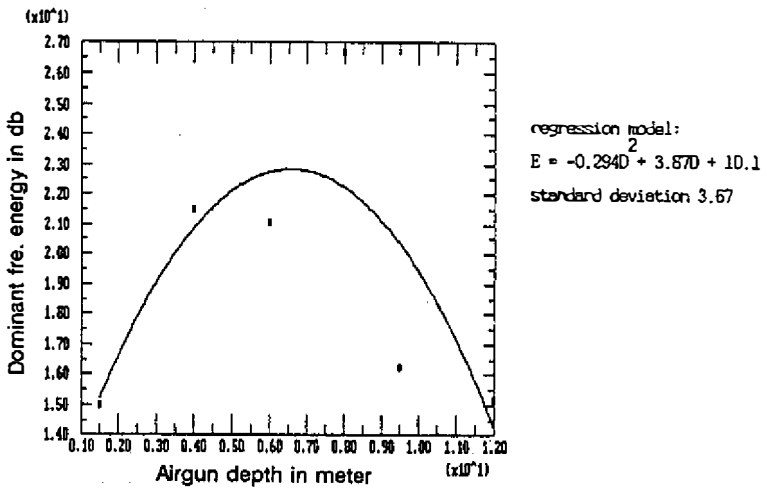

Fig. 15. Dominant frequency energy content E varying with airgun depth D (channel 11): $P = 1000\ psi$, $V = 1.4\ cu.in.$

to explain how airgun energy varies with the airgun depth. For airgun depth $D = 2\ m$, $t_s < 0.25\ T_i$ causes the major energy cancellation between initial pulse and ghost waves. For $D = 4\ m$, $T_i = 12\ msec$, and $t_s = 4.5\ msec$ which is $\leq 0.4\ T_i$, there is minor energy cancellation with major energy construction. For $D = 6,\ 8\ m$, $T_i > t_s > 0.5\ T_i$, there is no energy cancellation but energy construction. Therefore the receiving energy is increasing with an airgun depth ranging from 2 to 8 m, which is basically consistent with the observations of Brandsaeter *et al.* (1979).

Table 2. Initial pulse period (T_i), bubble period (T_b), and separation time (t_s) between direct and ghost waves recorded by channel 8.

Airgun depth	T_i	T_b	t_s
2 *m* *(1.5 *m*)	10 *msec*	20 *msec*	2 *msec*
4 *m* *(4.0 *m*)	12 *msec*	18 *msec*	4.5 *msec*
6 *m* *(6.0 *m*)	12 *msec*	17 *msec*	7.5 *msec*
8 *m* *(8.0 *m*)	13 *msec*	15.5 *msec*	10 *msec*
10 *m* *(9.5 *m*)	12 *msec*	14.5 *msec*	13.5 *msec*
12 *m* *(12.0 *m*)	11 *msec*	13 *msec*	15.0 *msec*

*airgun depth after correction

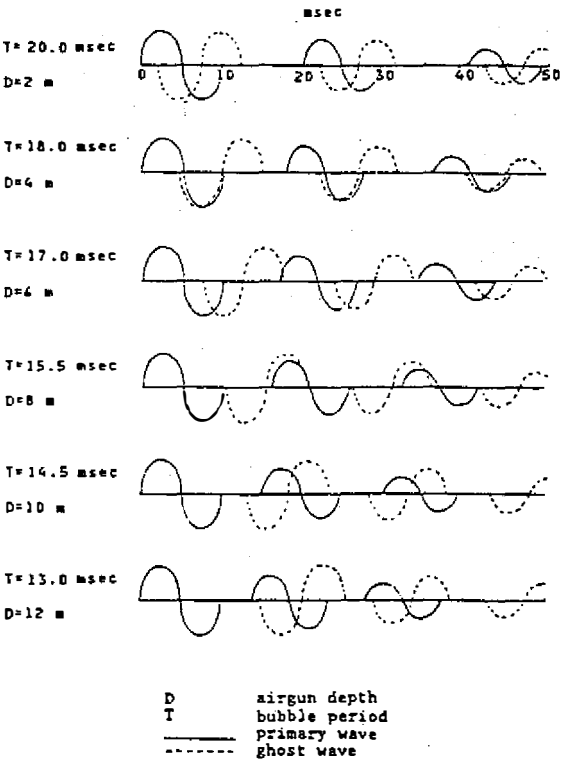

Fig. 16. Models of the ghost interference at different airgun depths *D*.

The ghost waves cancel out most of the direct bubble pulse energy and reinforce some of them when $D = 10,\ 12\ m$. In this experiment, the initial pressure pulse of $D = 12\ m$ is smaller than that of $D = 10\ m$ therefore the receiving energy is decreasing with airgun depths ranging from 8 to 12 m even though the ghost effect is about the same for both airgun depths of 10 and 12 m. This is in agreement with the experimental results reported by Mayne and Quay (1971).

5. CONCLUSIONS

This study has demonstrated that ghost interference plays an important role in the spectrum of airgun signatures. Some geophysicists (Vaage *et al.*, 1984) believe that the ghost signals usually do not affect the initial pulse as long as the airgun depth is greater than about 4 m. However, the initial pulse period for small airguns as used in this experiment is greater than 10 *msec* which indicates that the airgun depth should be deeper than 4 m to reduce ghost interference with the initial pulse. To choose an optimum airgun depth several factors need to be considered: signal resolution, penetration, afterflow effects, the cavitation problem, the dominant frequency range, and the noise coming from the hydrophone streamer (Larner *et al.*, 1981). For small airguns, 1.4 *cu.in.* for instance, an airgun depth of between 10 and 12 m is recommended because in addition to reducing the ghost interference and bubble pulses, the dominant frequency of the airgun signature also shifts to higher frequencies as the airgun depth increases (Table 1 and Eq.(1)). This is good for low frequency noise filtering because most of the major noises are in the seismic band below 60 Hz (Schoenberger and Mifsud, 1974). However, for a deep penetration seismic survey the low frequency band is preferred; therefore, one might have to make a compromise with the ghost interference and desired low frequency band.

Acknowledgments I thank Dr. J. J. Dowling of Marine Sciences Institute, University of Connecticut for help in assembling the equipment and collecting the field data. I also thank Dr. J. N. Gallagher of Amoco Production Research Center and Dr. G. Donathan for their helpful comments and constructive suggestions.

REFERENCES

Brandsaeter, H., Farestveit, A., and Ursin, B., 1979: A new high-resolution or deep penetration airgun array. *Geophysics*, **44**, no. 5, 865-879.

Dragoset, B., 1984: A comprehensive method for evaluation the design of airguns and airgun arrays. Presented at the 1984 Offshore Tech. Conf.

Fricke, J. R., Davis, J. M., and Reed, D. H., 1985: A standard quantitative calibration procedure for marine seismic sources. *Geophysics*, **50**, no. 10, 1525-1532.

Giles, B. F. and Johnston, R. C., 1973: System approach to airgun array design. *Geophysical Prospecting*, **21**, 77-101.

Hammond, J. W., 1962: Ghost elimination from reflection records. *Geophysics*, **27**, no. 1, 48-60.

Johnston, R. C., 1980: Performance of 2000 and 6000 p.s.i. airguns: Theory and experiment. *Geophysical Prospecting*, **28**, 700-715.

Jovanovich, D. B., Sumner, R. D., and Akins-Easterlin, S. L., 1983: Ghosting and marine signature deconvolution: A prerequisite for detailed seismic interpretation. *Geophysics*, **48**, no. 11, 1468-1485.

Kramer, F. S., Peterson, R. A., and Walter, W. C.(ed.), 1968: Seismic energy sources handbook. Presented at the 38th Ann. Mtg., Soc. Expl. Geophys.

Larner, K., Chambers, R., Yang, M., Lynn, W., and Wai, W., 1981: Coherent noise in marine seismic data. Presented at the 51st Ann. Mtg., Soc. Expl. Geophys.

Lindsey, J. P., 1960: Elimination of seismic ghost reflections by means of a linear filter. *Geophysics*, **25**, no. 1, 130-140.

Mayne, W. H. and Quay, R. G., 1971: Seismic signatures of large airguns. *Geophysics*, **36**, no. 6, 1162-1173.

Robinson, E. A. and Treitel, S., 1980: Geophysical signal analysis. Prentice-Hall, Inc., 466 pp.

Schneider, W. A., Larner, K. L., Burg, J. P., and Backus, M. M., 1964: A new data processing technique for the elimination of ghost arrivals on reflection seismograms. *Geophysics*, **29**, no. 5, 783-805.

Schoenberger, M., and Mifsud, J. F., 1974: Hydrophone streamer noise. *Geophysics*, **39**, 781-793.

Telford, W. M., Geldart, L. P., Sheriff, R. E., and Keys, D. A., 1976: Applied geophysics. Cambridge Univ. *Press*, 860 pp.

Vaage, S., Haugland, K., and Utheim, T., 1983: Signatures from single airguns. *Geophysical Prospecting*, **31**, 87-97.

Vaage, S., Ursin, B., and Haugland, K., 1984: Interaction between airguns. *Geophysical Prospecting*, **32**, 676-689.

鬼波干擾與空氣槍深度之設定

鄭懌

國立臺灣師範大學地球科學系

摘要

鬼波在震測中是一種無法避免的雜訊，尤其在海域震測，鬼波干擾更是嚴重。而鬼波之消除在震測資料處理上極爲耗時費力，因此在野外數據記錄時如何將鬼波干擾減至最低對爾後之資料處理幫助極大。本研究以小型空氣槍爲例，在不同深度下量取其特性信號，經由傅氏轉換後分析主頻帶能量分布。結果顯示鬼波干擾對震源能量之輸出有極大影響。主頻帶能量隨空氣槍深度之變化有類似拋物線之分布。此發現或許可解釋以往不同研究者間的衝突現象同時利用鬼波和氣泡脈衝之互相干擾可找出最佳之空氣槍置放深度，以獲得較適合之主頻帶頻域或較小之氣泡效應。